Hyper-spherical and Elliptical Stochastic Cycles

Luati, Alessandra and Proietti, Tommaso

Department of Statistics - University of Bologna, SEFEMEQ, University of Rome "Tor Vergata"

11 May 2009

Hyper-spherical and Elliptical Stochastic Cycles

Alessandra Luati
Department of Statistics
University of Bologna

Tommaso Proietti
S.E.F. e ME. Q.
University of Rome "Tor Vergata"

Abstract

A univariate first order stochastic cycle can be represented as an element of a bivariate first order vector autoregressive process, or VAR(1), where the transition matrix is associated with a Givens rotation. From the geometrical viewpoint, the kernel of the cyclical dynamics is described by a clockwise rotation along a circle in the plane. The reduced form of the cycle is either ARMA(2,1), with complex roots, or AR(1), when the rotation angle equals $2k\pi$ or $(2k+1)\pi, k = 0, 1, \ldots$.

This paper generalizes this representation in two directions. According to the first, the cyclical dynamics originate from the motion of a point along an ellipse. The reduced form is also ARMA(2,1), but the model can account for certain types of asymmetries. The second deals with the multivariate case: the cyclical dynamics result from the projection along one of the coordinate axis of a point moving in $\mathbb{R}^n$ along an hyper-sphere. This is described by a VAR(1) process whose transition matrix is obtained by a sequence of n-dimensional Givens rotations. The reduced form of an element of the system is shown to be ARMA(n, $n-1$). The properties of the resulting models are analyzed in the frequency domain, and we show that this generalization can account for a multimodal spectral density.

The illustrations show that the proposed generalizations can be fitted successfully to some well-known case studies of the econometric and time series literature. For instance, the elliptical model provides a parsimonious but effective representation of the mink-muskrat interaction. The hyper-spherical model provides an interesting re-interpretation of the cycle in US Gross Domestic Product quarterly growth and the cycle in the Fortaleza rainfall series.

Keywords: State space models; Predator-Prey Interaction; Givens Rotations.

1 Introduction

Modeling and interpreting cycles has attracted a great deal of attention in the time series literature. Many substantive applications can be found in diverse fields such as macroeconomics, biology, physics, meteorology and climatology.

Our current paradigm draws from the pioneering work of Yule (1927), who derived a stochastic cycle model by randomly shifting the amplitude and the phase of a deterministic cycle (a sine wave). Yule showed that this is equivalent to an autoregressive model, $\psi_t = 2\cos\omega\psi_{t-1} - \psi_{t-2} + \xi_t$, where $2\pi/\omega$ is the cycle period and ξ_t is a random source, i.e. a white noise process. Kendall (1945) provides an interesting review of early work on stochastic cycles, and further insight on the impact of this work on econometrics can be gained from Morgan (1990). Nonlinear extension have been provided by Tong and Lim (1980), whereas Gray, Zhang, and Woodward (1989) consider a fractionally integrated extension.

An alternative derivation of a stochastic cycle is based on a two-dimensional vector autoregressive model, describing the path of point on the plane whose position at time t is obtained by rotating counterclockwise by an angle ω its position at time $t-1$, and adding a a random perturbation. Damping is introduced by propagating only a constant proportion of the previous coordinates, so that the skeleton of the dynamic system eventually spirals down to the origin of the coordinate system. This framework is adopted by Harvey (1989) and West and Harrison (1989, 1997), and produces a marginal ARMA(2,1) process with pseudo-cyclical behavior for each of the two coordinates.

The paper proposes two extensions of the circular stochastic model. The first deals with an elliptical cycle model, which arises from the trajectory of a point on an ellipse. The second extension generalizes the idea in $n > 2$ dimensions and obtains the cyclical dynamics from the path of a point on a sphere or an hyper-sphere. This is achieved via a first order vector autoregressive model with transition matrix resulting from the product of matrices performing Givens rotations in a n-dimensional space. We show that the final equations form is ARMA$(n, n-1)$ and we provide a closed form expression for its spectral density. The relevance of these extensions is discussed using three empirical illustrations, the first concerning the estimation of the cyclical component in the growth rate of U.S. gross domestic product. The second deals with the series of rainfall at a location in Brazil. The third applies the elliptical cycle to model the mink-muskrat interaction.

The paper is organized as follows. Section 2 reviews in details the circular stochastic cycle model. The elliptical and higher dimensional extensions are developed in sections 3 and 4, respectively. Section 5 presents three main applications. In section 6 we discuss the results.

2 Circular stochastic cycles

A stochastic cycle model can be derived from the recursive representation of a deterministic cycle by a similar argument to that exploited by Yule (1927), who started from the homogeneous difference equation: $\psi_t - 2\rho\cos\omega\psi_{t-1} + \rho^2\psi_{t-2} = 0$, where $\omega \in [0,\pi]$ is the cycle frequency in radians, and introduced random disturbances on the right hand side, so as to obtain variation in the phase and the amplitude of the fluctuations. The approach taken by Hannan (1964) is to define a (seasonal) cycle as follows:

$$\psi_t = \alpha_t \cos\omega t + \alpha_t^* \sin\omega t,$$

where α_t and α_t^* are uncorrelated first order autoregressive processes; This process yields the variation in the phase and the amplitude of the fluctuations sought by Yule as it clear when it is rewritten as $\psi_t = A_t\cos(\omega t + \vartheta_t)$, where $A_t = (\alpha_t^2 + \alpha_t^{*2})^{1/2}$ is the random amplitude, and $\vartheta_t = \arctan(\alpha_t^*/\alpha_t)$ is the random phase in radians.

Harvey (1989) and West and Harrison (1989, 1997) use an alternative formulation, which defines ψ_t as an element of a bivariate vector autoregressive process:

$$\begin{bmatrix} \psi_t \\ \psi_t^\dagger \end{bmatrix} = \rho \begin{bmatrix} \cos\omega & \sin\omega \\ -\sin\omega & \cos\omega \end{bmatrix} \begin{bmatrix} \psi_{t-1} \\ \psi_{t-1}^\dagger \end{bmatrix} + \begin{bmatrix} \kappa_t \\ \kappa_t^\dagger \end{bmatrix}, \qquad (1)$$

where $\kappa_t \sim \mathrm{NID}(0,\sigma_\kappa^2)$ and $\kappa_t^\dagger \sim \mathrm{NID}(0,\sigma_\kappa^2)$ are mutually independent error terms, $\psi_t^\dagger$ is an auxiliary process which appears by construction in order to form ψ_t, measured in radians, and $\rho \in [0,1]$ is a damping factor. When $\rho = 1$, the skeleton describes the counterclockwise motion of a point along a circle in $\mathbb{R}^2$.

This model has been applied to macroeconomic time series by Harvey (1985) and Harvey and Jaeger (1993). Various modifications and extensions have been proposed in the literature: see, among others, Haywood and Tunnicliffe-Wilson (2000), Harvey and Trimbur (2003), Trimbur (2006).

The reduced form of (1) is the ARMA(2,1) process

$$(1 - 2\rho\cos\omega L + \rho^2 L^2)\psi_t = (1 - \rho\cos\omega L)\kappa_t + \rho\sin\omega\kappa_{t-1}^\dagger \qquad (2)$$

where L is the lag operator, $L^h y_t = y_{t-h}$. When ρ is strictly less than one the cycle is stationary with $\mathrm{E}(\psi_t) = 0$, $\mathrm{Var}(\psi_t) = \frac{\sigma_\kappa^2}{(1-\rho^2)}$, Corr $(\psi_t, \psi_{t-h}) = \rho^h\cos(h\omega)$, that can be easily calculated, as (1) is a VAR(1) process (Lütkepohl, 2006). The power spectrum is given by

$$f(\lambda) = \frac{\sigma_\kappa^2}{2\pi}\frac{1 + \rho^2 - 2\rho\cos\omega\cos\lambda}{1 + \rho^4 + 4\rho^2\cos^2\omega - 4\rho(1+\rho^2)\cos\omega\cos\lambda + 2\rho^2\cos(2\lambda)}. \qquad (3)$$

For ρ that tends to unity, the spectrum reaches its maximum at a frequency λ that tends to the frequency of the cycle, ω. As long as ρ decreases, the maximum of the spectrum is attained for values of $\lambda < \omega$, as stated in the following proposition, proved in Appendix A.

Proposition 1 *The maximum of the power spectrum (3) is attained for*

$$\lambda = \arccos\left\{\frac{1+\rho^2}{2\rho\cos\omega}\left(1 - \sin\omega\sqrt{1 - \frac{4\rho^2}{(1+\rho^2)^2}\cos^2\omega}\right)\right\}.$$

Henceforth, we shall refer to (1) as a circular stochastic cycle. From a geometrical point of view, the cycle dynamics are obtained clockwise rotation on a plane, around the origin, of the vector $\boldsymbol{\psi}_{t-1} = [\psi_{t-1} \ \ \psi^{\dagger}_{t-1}]'$ by the angle ω, damped through the factor ρ. The rotation is represented by the Givens matrix

$$\mathbf{G}(\omega) = \begin{bmatrix} \cos\omega & \sin\omega \\ -\sin\omega & \cos\omega \end{bmatrix}. \quad (4)$$

In fact, $\mathbf{G}(\omega)$ belongs to the special orthogonal group $SO(2)$, made of all the orthogonal matrices in $\mathbb{R}^2$ with determinant equal to one, i.e. $SO(2) = \{\mathbf{G} \in \mathbb{R}^{2\times 2}, \mathbf{G}^{-1} = \mathbf{G}', \det(\mathbf{G}) = 1\}$. Each time the vector $\boldsymbol{\psi}_{t-1}$ is rotated, it is contracted through the factor ρ, so to account for the dampening of the fluctuations, or zero long run persistence. The next two sections will deal with modifications and multivariate extensions of the circular model.

3 Elliptical stochastic cycles

Our first generalization deals with the shape of the cyclical component. In particular, we define the cyclical dynamics from the motion of a point along an ellipse in $\mathbb{R}^2$ rather than along a circle. According to the orientation of the ellipse, the model will be able to account for a faster or slower transition between positive and negative states. Letting $\alpha > 0, \beta > 0$ be two dilation coefficients, the path of a two-dimensional point that moves counterclockwise along an ellipse is obtained from a deterministic bivariate difference equation with transition matrix

$$\mathbf{E}(\omega) = \begin{bmatrix} \alpha & 0 \\ 0 & \beta \end{bmatrix} \mathbf{G}(\omega),$$

where $\mathbf{G}(\omega)$ is given in (4). The matrix $\mathbf{E}(\omega)$ performs the elliptical rotation by an angle ω; the dilation coefficients amplify or reduce the two coordinates.

The elliptical stochastic cycle is then defined as

$$\begin{bmatrix} \psi_t \\ \psi^{\dagger}_t \end{bmatrix} = \mathbf{E}(\omega) \begin{bmatrix} \psi_{t-1} \\ \psi^{\dagger}_{t-1} \end{bmatrix} + \begin{bmatrix} \kappa_t \\ \kappa^{\dagger}_t \end{bmatrix}, \quad (5)$$

with $\boldsymbol{\kappa}_t \sim \text{NID}(\mathbf{0}, \sigma^2_\kappa \mathbf{I})$. The reduced form of (5) is the ARMA(2,1) process

$$(1 - (\alpha+\beta)\cos\omega L + \alpha\beta L^2)\psi_t = (1 - \beta\cos\omega L)\kappa_t + \alpha\sin\omega\kappa^{\dagger}_{t-1}.$$

It is immediately clear that the stochastic cycle is stationary if $\alpha\beta < 1$ and $(\alpha+\beta)\cos\omega < 2$. The power spectrum is given by

$$f(\lambda) = \frac{\sigma^2_k}{2\pi} \frac{1 + \alpha^2\sin^2\omega + \beta^2\cos^2\omega - 2\beta\cos\omega\cos\lambda}{1 + \alpha^2\beta^2 + (\alpha+\beta)^2\cos^2\omega - 2(\alpha+\beta)(1+\alpha\beta)\cos\omega\cos\lambda + 2\alpha\beta\cos(2\lambda)}. \quad (6)$$

When $\alpha = \beta = \rho$ we find the first order stochastic cycle (1), with spectrum (3). If $\beta = \frac{1}{\alpha} = \frac{1}{cos\omega} - \tan\omega$, then the autoregressive polynomial has unit roots and the cycle is nonstationary. Note that in this case, $\alpha = \frac{1}{cos\omega} + \tan\omega$ and $\alpha\beta = 1$, $(\alpha + \beta)\cos\omega = 2$. For this (α, β) pair, if one switches off the shocks, i.e $\kappa_t = \kappa_t^\dagger = 0, \forall t$, then equation (5) describes the deterministic motion along an ellipse. As a matter of fact, the cartesian coordinates of a point on an ellipse of equation $\frac{\psi_t^2}{\alpha^2} + \frac{\psi_t^{\dagger 2}}{\beta^2} = 1$, and centered at the origin, are $\psi_t = \alpha\cos(\omega t)$ and $\psi_t^\dagger = \beta\sin(\omega t)$, where ω is the angle between the axis α (β) and the auxiliary circle of radius equal to α (β), representing the position of a point moving along the ellipse. The factors α and β account for an asymmetric dampening of the fluctuations and either α or β can assume value equal to one (or greater). For $\alpha, \beta \to 1$ the spectral power of the cycle (5) is more concentrated near the spectral peak than the cycle (1) when $\rho \to 1$.

Proposition 2 *The maximum of the power spectrum (6) is attained for*

$$\lambda_{max} = \arccos\left\{\frac{1 + R^2}{2\beta\cos\omega}\left(1 - \sin\omega\sqrt{1 - \frac{G}{(1 + R^2)^2}\cos^2\omega}\right)\right\},$$

where $R^2 = \alpha^2\sin^2\omega + \beta^2\cos^2\omega$ *and* $G = \frac{1}{\sin^2\omega}[(1 + R^2)(1 + \alpha\beta + \frac{\beta}{\alpha} + \beta^2) - \frac{\beta}{\alpha}((1 - \alpha\beta)^2 + \cos^2(\omega)(\alpha + \beta)^2) - (1 + R^2)^2]$.

If $\alpha = \beta = \rho$, then $(1 + R^2) = 1 + \rho^2$ and $G = 4\rho^2$, hence, we find Proposition 1. Furthermore, as long as either α or β are different than one, the maximum of the spectrum is closer to ω for $\beta > \alpha$ than for $\beta < \alpha$.

The elliptical model can also be used as a model for bivariate cycles, in which case we $\boldsymbol{\kappa}_t \sim \text{NID}(\mathbf{0}, \boldsymbol{\Sigma})$. In section 5.3 we will illustrate its use for modeling the predator-prey cycles characterizing a bivariate population.

4 Multivariate extensions

This section deals with the extension of the circular model to the dynamics of a point along a sphere in $\mathbb{R}^3$ and an hyper-sphere in $\mathbb{R}^n$.

4.1 Spherical stochastic cycles

Rotations in the three dimensional Euclidean space are completely specified by three angles, known as Euler angles (Goldstein, 1980, §4-4). In fact, according to Euler theorem, any rotation in $\mathbb{R}^3$ can be carried out by means of three successive rotations, each one about a specific axis, performed in some sequence. The Euler angles are then defined as the three successive angles of rotation. Let us denote the Euler angles by θ, ϕ and ω. Then, rotations around the x, y, z axes with frequencies θ, ϕ, ω, are represented, respectively, by the rotation matrices $\mathbf{G}_x(\theta), \mathbf{G}_y(\phi), \mathbf{G}_z(\omega) \in SO(3)$ defined as

$$\mathbf{G}_x(\theta) = \begin{bmatrix} 1 & 0 & 0 \\ 0 & \cos\theta & \sin\theta \\ 0 & -\sin\theta & \cos\theta \end{bmatrix},$$

$$\mathbf{G}_y(\phi) = \begin{bmatrix} \cos\phi & 0 & \sin\phi \\ 0 & 1 & 0 \\ -\sin\phi & 0 & \cos\phi \end{bmatrix},$$

and

$$\mathbf{G}_z(\omega) = \begin{bmatrix} \cos\omega & \sin\omega & 0 \\ -\sin\omega & \cos\omega & 0 \\ 0 & 0 & 1 \end{bmatrix}.$$

The elements of a complete rotation can be therefore obtained by writing the associated matrix as the triple product of the above three matrices. As an illustration, let us consider the so called x-convention (see Goldstein, 1980), according to which the first rotation is carried out by an angle $\omega \in [0, 2\pi]$ about the z-axis, the second rotation is by an angle $\theta \in [0, \pi]$ about the x-axis, and the third rotation is by an angle $\phi \in [0, 2\pi]$ about the z-axis, i.e. $\mathbf{G}_{zxz}(\omega, \theta, \phi) = \mathbf{G}_z(\omega)\mathbf{G}_x(\theta)\mathbf{G}_z(\phi)$, i.e.

$$\mathbf{G}_{zxz}(\omega, \theta, \phi) = \begin{bmatrix} \cos\phi\cos\omega - \cos\theta\sin\omega\sin\phi & \cos\phi\sin\omega + \cos\theta\cos\omega\sin\phi & \sin\phi\sin\theta \\ -\sin\phi\cos\omega - \cos\theta\sin\omega\cos\phi & -\sin\phi\sin\omega + \cos\theta\cos\omega\cos\phi & \cos\phi\sin\theta \\ \sin\theta\sin\omega & -\sin\theta\cos\omega & \cos\theta \end{bmatrix}.$$

In the following, we shall drop the subscripts indicating the axes of rotation and denote a rotation matrix parametrised by Euler angles as $\mathbf{G}(\omega, \theta, \phi)$. The determinant of $\mathbf{G}(\omega, \theta, \phi)$ is equal to one, the inverse coincides with the transpose, and the spectrum is the set $\{1, e^{\imath\xi}, e^{-\imath\xi}\}$, where $\imath$ is the imaginary unit, and

$$\xi = \arccos\left\{\frac{1}{2}\left(\mathrm{tr}\left(\mathbf{G}(\omega, \theta, \phi)\right) - 1\right)\right\}$$

is the overall rotation angle around the eigenvector associated with the eigenvalue equal to one (Goldstein, 1980, pag. 162). By means of some (unitary) similarity transformation, it is always possible to transform any rotation matrix like $\mathbf{G}(\omega, \theta, \phi)$, to a system of coordinates where the z axis lies along the axis of rotation. Specifically,

$$\mathbf{G}_z(\xi) = \mathbf{Z}\mathbf{G}(\omega, \theta, \phi)\mathbf{Z}' \tag{7}$$

where $\mathbf{Z} = \mathbf{Q}\mathbf{P}^H$ and the columns of $\mathbf{Q}$ and $\mathbf{P}$ are the eigenvectors of $\mathbf{G}_z(\xi)$ and $\mathbf{G}(\omega, \theta, \phi)$, respectively; the superscript ^{H} stands for hermitian transposition. That $\mathbf{P}$ and $\mathbf{Q}$ are unitary matrices follows by the fact that $\mathbf{G}_z(\xi)$ and $\mathbf{G}(\omega, \theta, \phi)$ are normal (see Meyer, 2000, § 7.5); the product matrix $\mathbf{Z}$ is orthogonal, i.e. $\mathbf{Z}^{-1} = \mathbf{Z}' = \mathbf{P}\mathbf{Q}^H$, and its elements are denoted by $z_{ij},\ i, j = 1, 2, 3$.

Against this background, we specify a three-dimensional first order stochastic cycle as follows:

$$\begin{bmatrix} \psi_t \\ \psi_t^{\dagger} \\ \psi_t^{\ddagger} \end{bmatrix} = \rho \mathbf{G}(\omega,\theta,\phi) \begin{bmatrix} \psi_{t-1} \\ \psi_{t-1}^{\dagger} \\ \psi_{t-1}^{\ddagger} \end{bmatrix} + \begin{bmatrix} \kappa_t \\ \kappa_t^{\dagger} \\ \kappa_t^{\ddagger} \end{bmatrix}, \tag{8}$$

or, in matrix form, $\boldsymbol{\psi}_t = \rho\mathbf{G}(\omega,\theta,\phi)\boldsymbol{\psi}_{t-1} + \boldsymbol{\kappa}_t$, where $\boldsymbol{\kappa}_t$ is a zero mean process with covariance matrix $\boldsymbol{\Sigma}_\kappa$ and $\rho \in [0,1)$. The latter condition ensures that the VAR(1) process (8) is stationary, which follows by the fact that the eigenvalues of $\mathbf{G}(\omega,\theta,\phi)$ are all in modulus equal to one. Hence, for $\rho < 1$ and $\boldsymbol{\Sigma}_\kappa = \sigma_\kappa^2\mathbf{I}$, the stationary process (8) has zero mean and covariance matrix $\boldsymbol{\Sigma}_\psi(0) = \frac{\sigma_\kappa^2}{(1-\rho^2)}\mathbf{I}$, satisfying the matrix equation $\boldsymbol{\Sigma}_\psi(0) = \rho^2\mathbf{G}(\omega,\theta,\phi)\boldsymbol{\Sigma}_\psi(0)\ \mathbf{G}(\omega,\theta,\phi)' + \boldsymbol{\Sigma}_\kappa$, in the light of the orthogonality of $\mathbf{G}(\omega,\theta,\phi)$ and the fact that $\boldsymbol{\Sigma}_\kappa$ is scalar. Under these assumptions, the reduced form of (8) can be conveniently derived using the ξ parametrization (7), holding for any choice of Euler angles and axes of rotation.

Proposition 3 *The reduced form of ψ_t in (8) is the stationary ARMA(3,2) process*

$$\begin{aligned} (1-\rho L)(1-2\rho\cos\xi L+\rho^2L^2)\psi_t &= (1-\rho L)(z_{11}(1-\cos\xi\rho L) - z_{21}\sin\xi\rho L)\kappa_t + \\ &\quad +(1-\rho L)(z_{11}\sin\xi\rho L + z_{21}(1-\cos\xi\rho L))\kappa_t^{\dagger} + \\ &\quad +z_{31}(1-2\rho\cos\xi L+\rho^2L^2)\kappa_t^{\ddagger}, \end{aligned} \tag{9}$$

with spectrum

$$f(\lambda) = \frac{\sigma_\kappa^2}{2\pi}\left(\frac{(1+\rho^2)z_1 + \rho^2 z_2\sin(2\xi) - 2\rho\cos\lambda(z_1\cos\xi - z_2\sin\xi)}{1+\rho^4+4\rho^2\cos^2\omega - 4\rho(1+\rho^2)\cos\omega\cos\lambda + 2\rho^2\cos(2\lambda)} + \frac{z_3}{1-2\rho\cos\lambda+\rho^2}\right),$$

where we have set $z_1 = z_{11}^2 + z_{21}^2$, $z_2 = 2z_{11}z_{21}$ and $z_3 = z_{31}^2$.

In proving proposition 3 (Appendix C), we show that the transformation represented by $\mathbf{Z}$ makes the cycle defined in (8) observationally equivalent to the bivariate first order stochastic cycle (1). The reduced form of the first component of $\mathbf{Z}\boldsymbol{\psi}_t$ is in fact the ARMA(2,1) process (2).

Note that, whatever the choice of the axes of rotation, if $\theta = \phi = 0$, then $\mathbf{Z} = \mathbf{I}$, $\xi = \omega$ and we find the reduced form (2) and the spectrum (3) of the first order stochastic cycle (1). Specific choices of the axes of rotation give rise to different conditions for (8) to become observationally equivalent to (1). For example, in the x-convention, where rotations are represented by $\mathbf{G}_{zxz}(\omega,\theta,\phi)$, if $\theta = 0$, then $\mathbf{Z}$ is the identity matrix and the reduced form of ψ_t is equal to that of the first order stochastic cycle (1) with frequency $\xi = \omega + \phi$.

The more general representation provided by (8) gives rise to spectral densities that may be more concentrated around the maximum (with respect to the circular case) and/or may display two modes with one mode located at the zero frequency.

4.2 A general model for n-dimensional cycles

The natural generalization of models (1) and (8) to higher dimensions is obtained by means of Givens rotations (Givens, 1958), performed by orthogonal matrices of the form:

$$
\mathbf{G}_{ij}(\omega) = \begin{array}{c} \begin{array}{ccccccc} & & \text{col } i & & \text{col } j & & \\ & & \downarrow & & \downarrow & & \end{array} \\ \begin{bmatrix} 1 & \dots & 0 & \dots & 0 & \dots & 0 \\ \vdots & \ddots & \vdots & & \vdots & & \vdots \\ 0 & \dots & \cos\omega & \dots & \sin\omega & \dots & 0 \\ \vdots & & \vdots & \ddots & \vdots & & \vdots \\ 0 & \dots & -\sin\omega & \dots & \cos\omega & \dots & 0 \\ \vdots & & \vdots & & \vdots & \ddots & \vdots \\ 0 & \dots & 0 & \dots & 0 & \dots & 1 \end{bmatrix} \end{array} \begin{array}{l} \\ \\ \\ \\ \leftarrow \text{row } i \\ \\ \leftarrow \text{row } j \\ \\ \\ \end{array}
$$

for $i, j = 1, 2, \dots, n$ (see Golub and van Loan, 1996, § 5.1.8 and Meyer, 2000, § 5.6). Premultiplication of an n-dimensional vector by $\mathbf{G}_{ij}(\omega)$ corresponds to a rotation of ω radians in the (i, j)-th coordinate plane. Note that $\mathbf{G}(\omega)$ and the set $\mathbf{G}_x(\theta)$, $\mathbf{G}_y(\phi)$, $\mathbf{G}_z(\omega)$ are Givens rotations in $\mathbb{R}^2$ and $\mathbb{R}^3$, respectively. To perform a complete n-dimensional rotation of a given vector, $\binom{n}{2}$ products must be computed, while a rotation around one specified axis requires $n-1$ products. For example, let us consider $\mathbb{R}^4$, for which up to six Givens matrices are defined. A complete rotation is obtained by rotating all the coordinates of the vector $\boldsymbol{\psi}_t = [\psi_{t,1} \;\; \psi_{t,2} \;\; \psi_{t,3} \;\; \psi_{t,4}]'$ through the product of the matrices $\mathbf{G}_{12}, \mathbf{G}_{13}, \mathbf{G}_{14}, \mathbf{G}_{23}, \mathbf{G}_{24}, \mathbf{G}_{34}$ according to some order (we have omitted the angles for sake of notation). On the other hand, a rotation around the first coordinate axis, which remains fixed, is obtained by multiplications of $\mathbf{G}_{23}, \mathbf{G}_{24}, \mathbf{G}_{34}$.

The model for an hyper-spherical n-dimensional stochastic cycle $\boldsymbol{\psi}_t$ is defined as follows:

$$
\boldsymbol{\psi}_t = \rho \mathbf{G}(\boldsymbol{\omega}) \boldsymbol{\psi}_{t-1} + \boldsymbol{\kappa}_t \tag{10}
$$

provided that $\boldsymbol{\psi}_{t-1}$ and $\boldsymbol{\kappa}_t$ are n-dimensional vectors, ρ is scalar and with

$$
\mathbf{G}(\boldsymbol{\omega}) = \prod_{i=1,\, j \geq i+1}^{n-1} \mathbf{G}_{ij}(\omega_{ij}) \tag{11}
$$

where the matrices entering in the product can be taken in any order and $\boldsymbol{\omega} = (\omega_{12}, \omega_{13}, \dots, \omega_{n-1,n})$ is the parameter vector, containing up to $\binom{n}{2}$ different angles. We allow some but not all of the ω_{ij} to be equal to zero, i.e. $\omega_{ij} \in [0, \pi)$ provided that $\boldsymbol{\omega} \neq \mathbf{0}$.

Assuming that $\rho \in (0, 1)$ and that the components of $\boldsymbol{\kappa}_t$ are uncorrelated error terms with zero mean and constant variance equal to σ^2_κ, equation (10) specifies a general model for a stationary stochastic cycle that encompasses (1) and (8) as particular cases where results can be obtained in closed form as functions of the rotation angles. In fact, (1) is a trivial example of (10) in $\mathbb{R}^2$ while (8) is the most general case of (10) in $\mathbb{R}^3$, since it enables a full specification of the rotation angles and sequence of rotation axes.

Proposition 4 *The reduced form of $\psi_{t,1}$ in (10) is an ARMA($n, n-1$) process. Specifically, for $n \geq 2$, n even,*

$$\prod_{h=1}^{\frac{n}{2}} (1 - 2\rho \cos \zeta_h L + \rho^2 L^2)\psi_{t,1} = -\sum_{j=1}^{n}\sum_{i=1}^{n}\sum_{k=1}^{n} (-1)^{n-j} s_{n-j} v_{1i} (1 - \rho e^{\imath \zeta_i} L)^{j-1} \overline{v}_{ki} \kappa_{t,k} \tag{12}$$

and, for $n \geq 3$, n odd,

$$(1 - \rho L) \prod_{h=1}^{\frac{n-1}{2}} (1 - 2\rho \cos \zeta_h L + \rho^2 L^2)\psi_{t,1} = \sum_{j=1}^{n}\sum_{i=1}^{n}\sum_{k=1}^{n} (-1)^{n-j} s_{n-j} v_{1i} (1 - \rho e^{\imath \zeta_i} L)^{j-1} \overline{v}_{ki} \kappa_{t,k}, \tag{13}$$

where $s_{n-j} = \sum_{1 \leq i_1 < i_2 < \ldots < i_{n-j} \leq n} (1 - \rho e^{\imath \zeta_{i_1}} L)(1 - \rho e^{\imath \zeta_{i_2}} L) \ldots (1 - \rho e^{\imath \zeta_{i_{n-j}}} L)$, v_{ki} is the generic element of $\mathbf{V}$, $\overline{v}_{ki}$ is its complex conjugate and the columns of $\mathbf{V}$ are eigenvectors of $\mathbf{G}(\boldsymbol{\omega})$ associated with the eigenvalues $\{e^{\imath \zeta_1}, e^{\imath \zeta_2}, \ldots, e^{\imath \zeta_n}\}$, where $\zeta_{2h} = -\zeta_{2h-1}$, for $h = 1, 2, \ldots, \frac{n-1}{2}$, and $\zeta_n = 0$ if n is odd. The spectra of (12) and (13) are given, respectively, by

$$f(\lambda) = \frac{\sigma_\kappa^2}{2\pi} \frac{\sum_{k=1}^{n} \left| -\sum_{j=1}^{n} \sum_{i=1}^{n} \sum_{1 \leq i_1 < \ldots < i_{n-j} \leq n} \prod_{l=1}^{n-j} (1 - \rho e^{\imath \zeta_{i_l} + \lambda}) v_{1i} (1 - \rho e^{\imath \zeta_i + \lambda})^{j-1} \overline{v}_{ki} \right|^2}{\prod_{h=1}^{\frac{n}{2}} (1 + \rho^4 + 4\rho^2 \cos^2 \zeta_h - 4\rho(1 + \rho^2) \cos \zeta_h \cos \lambda + 2\rho^2 \cos(2\lambda))} \tag{14}$$

and

$$f(\lambda) = \frac{\sigma_\kappa^2}{2\pi} \frac{\sum_{k=1}^{n} \left| \sum_{j=1}^{n} \sum_{i=1}^{n} \sum_{1 \leq i_1 < \ldots < i_{n-j} \leq n} \prod_{l=1}^{n-j} (1 - \rho e^{\imath \zeta_{i_l} + \lambda}) v_{1i} (1 - \rho e^{\imath \zeta_i + \lambda})^{j-1} \overline{v}_{ki} \right|^2}{(1 - 2\rho \cos \lambda + \rho^2) \prod_{h=1}^{\frac{n-1}{2}} (1 + \rho^4 + 4\rho^2 \cos^2 \zeta_h - 4\rho(1 + \rho^2) \cos \zeta_h \cos \lambda + 2\rho^2 \cos(2\lambda))}. \tag{15}$$

Notice that s_{n-j} is a polynomial of degree $n - j$ in the lag operator L (see the proof in Appendix D), whereas both the left hand sides of (12) and (13) feature a polynomial of order n in L. Hence, the reduced form of $\psi_{t,1}$ in (10) is an ARMA($n, n-1$) process, whose coefficients depend on the eigenvalues of $\mathbf{G}(\boldsymbol{\omega})$. In terms of the angles of rotations, (12) and (13) are given in (2) and (9) for $n = 2$ and $n = 3$, respectively.

Equation (10) describes a very general model. Due to the variety of combinations of angles and products that generate $\mathbf{G}(\boldsymbol{\omega})$, it is practically impossible to formulate equations (12-13) and (14-15) explicitly as trigonometric functions of the original rotation angles. However, once fixed (or estimated) the angles and the factors in $\mathbf{G}(\boldsymbol{\omega})$, then the eigenvalues of $\mathbf{G}(\boldsymbol{\omega})$ can be analytically obtained as functions of the rotation angles and, consequently, reduced forms and spectra can be obtained in a closed form.

A special case occurs when the ζ_h's are the same in modulus, i.e. is $\zeta_h = \pm\zeta$ (except for $\zeta_n = 0$, when n is odd). In this special case, (12) and (13) collapse to the circular and spherical case, respectively, due to the presence of common factors in the AR and MA polynomials. A necessary and sufficient condition for $\zeta_h = \pm\zeta,\ \forall h$ (except the last if n is odd) is

$$\mathbf{G}(\boldsymbol{\omega}) + \mathbf{G}'(\boldsymbol{\omega}) = 2\cos\zeta\mathbf{I} \tag{16}$$

if n is even, or

$$\mathbf{G}(\boldsymbol{\omega}) + \mathbf{G}'(\boldsymbol{\omega}) = \begin{bmatrix} 2\cos\zeta\mathbf{I} & 0 \\ 0 & 2 \end{bmatrix} \tag{17}$$

if n is odd. In fact, if n is even (and in the following we shall consider only this case for brevity) and $\zeta_h = \zeta,\ \forall h$, it follows from the spectral decomposition $\mathbf{G}(\boldsymbol{\omega}) = \mathbf{V}\boldsymbol{\Xi}\mathbf{V}^H$ that $\mathbf{G}(\boldsymbol{\omega}) + \mathbf{G}'(\boldsymbol{\omega}) = \mathbf{V}(\boldsymbol{\Xi} + \boldsymbol{\Xi}^H)\mathbf{V}^H = 2\cos\zeta\mathbf{I}$, as $\boldsymbol{\Xi} + \boldsymbol{\Xi}^H = 2\cos\zeta\mathbf{I}$ and $\mathbf{V}$ is unitary. On the other hand, if $\mathbf{G}(\boldsymbol{\omega}) + \mathbf{G}'(\boldsymbol{\omega}) = 2\cos\zeta\mathbf{I}$, then using again the spectral decomposition and observing that the generic element of $\boldsymbol{\Xi} + \boldsymbol{\Xi}^H$ is $2\cos\zeta_h$, it follows that $2\cos\zeta_h = 2\cos\zeta,\ \forall h$. Hence, $\cos\zeta_h = \cos\zeta$, i.e, in $[0, 2\pi)$, $\zeta_h = \zeta$.

In conclusion, the model (10) nests the $n = 2$ circular model when n is even, and the spherical model when n is odd. A trivial example is when $\mathbf{G}(\omega)$ is the the block diagonal matrix $\mathbf{G}(\omega) = \mathbf{G}_{12}(\omega)\mathbf{G}_{34}(\omega)\dots\mathbf{G}_{n-1,n}(\omega)$, depending on the single parameter ω, in which case $\zeta = \omega$. When the transition matrix is specified as (11), a necessary condition for $\zeta_h = \pm\zeta$ is to choose $\omega_{ij} = \omega + j\pi$. For instance, for $n = 4$ and $\mathbf{G}(\omega) = \mathbf{G}_{12}(\omega)\mathbf{G}_{13}(\omega+\pi)\mathbf{G}_{14}(\omega+2\pi)\mathbf{G}_{23}(\omega+3\pi)\mathbf{G}_{24}(\omega+4\pi)\mathbf{G}_{34}(\omega+5\pi)$, we have $\cos\zeta = -\cos^3\omega$, so that $\mathbf{G}(\omega) - \cos\zeta\mathbf{I}$ is antisymmetric and $\mathbf{G}(\omega)$ satisfies (16).

Model (10) can also be used as a multivariate cycle model that captures the interactions within a system of observed time series, in which case we would change specification for the covariance matrix of the cycle disturbances, by letting $\boldsymbol{\kappa}_t \sim \mathrm{N}(\mathbf{0}, \boldsymbol{\Sigma})$. The spectral analysis of the model properties is carried out through the multivariate spectrum $\mathbf{F}(\lambda)$, that is the matrix with diagonal elements $f_{ii}(\lambda)$ equal to the power spectra of the components $\psi_{t,i}$ and off-diagonal elements $f_{ij}(\lambda)$ that are the cross-spectra between the i-th and j-th components at the frequency λ. Using the spectral generating function of a VAR(1) model, we have that the multivariate spectrum of the process (10) is given by

$$\mathbf{F}(\lambda) = \frac{1}{2\pi}\left[\mathbf{I} - \rho\mathbf{G}(\boldsymbol{\omega})e^{-\imath\lambda}\right]^{-1}\boldsymbol{\Sigma}_\kappa\left[\mathbf{I} - \rho\mathbf{G}'(\boldsymbol{\omega})e^{\imath\lambda}\right]^{-1}. \tag{18}$$

. Using standard algebra and some results contained in the proof of proposition 3, we find that

$$f_{ij}(\lambda) = \frac{\sum_{k=1}^n a_{i,k}(\lambda)\sum_{l=1}^n \sigma_{kl}\bar{a}_{j,l}(\lambda)}{2\pi d(\lambda)}, \quad i,j = 1,\dots,n$$

where $a_{i,k}(\lambda) = \sum_{p=1}^n (-1)^{n-p}s_{n-p}\sum_{q=1}^n v_{iq}(1-\rho e^{\imath(\zeta_q-\lambda)})^{p-1}\bar{v}_{kq}$, v_{iq} and s_{n-p} are defined in proposition 3, σ_{ij} is the generic element of $\boldsymbol{\Sigma}_\kappa$ and $d(\lambda) = \prod_{h=1}^{\frac{n}{2}}(1+\rho^4+4\rho^2\cos^2\zeta_h - 4\rho(1+\rho^2)\cos\zeta_h\cos\lambda + 2\rho^2\cos(2\lambda))$ if n is even or $d(\lambda) = (1-2\rho\cos\lambda+\rho^2)\prod_{h=1}^{\frac{n-1}{2}}(1+\rho^4+4\rho^2\cos^2\zeta_h - 4\rho(1+\rho^2)\cos\zeta_h\cos\lambda + 2\rho^2\cos(2\lambda))$ if n is odd. By construction, $f_{ji}(\lambda)$ is the complex conjugate of $f_{ij}(\lambda)$.

The coherence spectrum $c^2(\lambda)$ and the phase $\phi(\lambda)$ are

$$c^2(\lambda) = \frac{f_{ij}(\lambda)f_{ji}(\lambda)}{f_{ii}(\lambda)f_{jj}(\lambda)} \quad \text{and} \quad \phi(\lambda) = \text{ arctan } \left\{ \frac{\Im f_{ij}(\lambda)}{\Re f_{ij}(\lambda)} \right\}$$

for $i, j = 1, 2, \ldots, n$ and where $\Re$ and $\Im$ denote the real and imaginary part of a complex number.

5 Illustrations

The proposed generalizations will now be used for extracting cycles in three well known time series that have been analyzed extensively in the literature and that provide a useful testbed for our models.

For statistical treatment, the cycle models parameterize components of a more general state space model, that can be estimated by maximum likelihood using the support of the Kalman filter. Conditional on the maximum likelihood parameter estimates, a smoothing algorithm delivers the minimum mean square estimates of the cycle conditional on the available observations. See Harvey (1989) and Durbin and Koopman (2001) for a full account of the methodology. Model selection is carried out by an information criterion, such as AIC or BIC. All the computations have been carried out in Ox 4.00 by Doornik (2006).

5.1 US Gross Domestic Product

Our first illustration concerns the quarterly growth rate of real gross domestic product (GDP) for the U.S., available for the sample period 1947:2-2008:4. The series is plotted in the top left hand panel of figure 1. We fit the cycle plus irregular model: $y_t = \mu + \psi_t + \epsilon_t$, where μ is a constant, $\epsilon_t \sim \text{WN}(0, \sigma^2_\epsilon)$ and ψ_t is the generalized n-dimensional cyclical component given in (10)-(11).

Table 1 presents the results of fitting cycle models of different dimension. The first ($n = 2$) is the circular model described in (1); for the three-dimensional spherical model ($n = 3$) we consider the specification with $\mathbf{G}(\boldsymbol{\omega}) = \mathbf{G}_{12}(\omega)\mathbf{G}_{13}(\omega)\mathbf{G}_{23}(\omega)$, i.e. the same rotation angle defines the three Givens matrices, and the specification with three different angles ($k = 3$), so that $\mathbf{G}(\boldsymbol{\omega}) = \mathbf{G}_{12}(\omega_1)\mathbf{G}_{13}(\omega_2)\mathbf{G}_{23}(\omega_3)$. Finally, we present the results for the four dimensional model with only one rotation angle ($n = 4, k = 1$), with six rotation angles, $n = 4, k = 6$, that is the model with transition matrix proportional to $\mathbf{G}(\boldsymbol{\omega}) = \mathbf{G}_{12}(\omega_1)\mathbf{G}_{13}(\omega_2)\mathbf{G}_{14}(\omega_3)\mathbf{G}_{23}(\omega_4)\mathbf{G}_{24}(\omega_5)\mathbf{G}_{34}(\omega_6)$, along with a more parsimonious specification with only $k = 3$ rotation angles, having

$$\mathbf{G}(\boldsymbol{\omega}) = \mathbf{G}_{12}(\omega_1)\mathbf{G}_{13}(\omega_2)\mathbf{G}_{14}(\omega_1)\mathbf{G}_{23}(\omega_3)\mathbf{G}_{24}(\omega_2)\mathbf{G}_{34}(\omega_3).$$

The specifications $n = 4, k = 3$ and $n = 4, k = 6$ yield exactly the same performance, and since the former is more parsimonious, it is preferred by the two information criteria. The model $n = 4, k = 3$

Model	$\hat{\rho}$	$\hat{\omega} \in (0, \pi)$	$10^7 \hat{\sigma}_\kappa^2$	$10^7 \hat{\sigma}_\epsilon^2$	log-likelihood	AIC	BIC	Ljung-Box (8)
$n = 2$	0.78	0.54	188	472	916.27	-1822.3	-1805.1	2.79
$n = 3, k = 1$	0.82	0.38	153	492	916.16	-1822.1	-1804.8	4.35
$n = 3, k = 3$	0.80	0.39;0.39;0.25	171	481	916.31	-1818.2	-1794.2	3.27
$n = 4, k = 1$	0.84	0.30	138	503	915.82	-1821.4	-1804.2	5.50
$n = 4, k = 3$	0.94	0.37; 0.19; 0.42	48	561	919.16	-1823.8	-1799.9	3.93
$n = 4, k = 6$	0.94	0.35; 0.23; 0.35	48	561	919.16	-1817.5	-1783.4	3.93
		0.43; 0.13; 0.43						

Table 1: U.S. GDP quarterly growth. Estimation results

has the highest likelihood and the smallest AIC, and thus it would be selected according to this criterion. However, the $n = 2$ cycle is the best specification according to the BIC.

Figure 1 displays (top right panel) the sample spectrum and the parametric spectra implied by the $n = 2$ and $n = 4, k = 3$ models. The former peaks at a period of about 3 years. The second has two peaks at the spectral frequencies $\hat{\zeta}_1 = 0.30$ and $\hat{\zeta}_2 = 0.69$, corresponding to a five-year cycle and to a short-run cycle with period of about two years. Although the smoothed estimates of the two cyclical components do not differ dramatically (the $n = 4$ resulting somewhat smoother), we think that the interpretation of the bimodal spectrum is interesting. In the light of (12), the four dimensional cycle results from the sum of two cyclical components, the first, with ζ_1 close to 0.1π, describing a five-year cycle, the second, with frequency corresponding to 2 years, describing a short-run cycle. The bottom right panel of figure 1, shows that the two-year plays a prominent role in the first part of the series, but then reduces prominently its amplitude. The five-year cycle plays a more important role at the end of the sample.

The presence of a two-year cycle has been attested in the literature. For instance, the ARIMA(2,1,2) estimated by Morley, Nelson and Zivot (2003) for the same series implies a cycle of 2.4 years.

5.2 Rainfall in Fortaleza

The series is the annual record of the number of centimeters of rainfall at Fortaleza, Brazil, for the period 1849-1992 (Source: Koopman et al., 2006). It provides an interesting case study for the detection and modelling of cycles in rainfall. Harvey and Souza (1987, HS) proposed the model

$$y_t = \mu + \psi_{1t} + \psi_{2t} + \epsilon_t,$$

where $\epsilon_t \sim \text{WN}(0, \sigma_\epsilon^2)$ and $\psi_{it}, i = 1, 2$, are two independent cycles specified as in (1). Maximum likelihood estimation (for the sample period up to 1979) gave two deterministic cycles with period 13 and 26 years; diagnostic checking and goodness of fit assessment led to conclude that the model provided a satisfactory representation of the data; moreover, the presence of two deterministic cycles is a fact well documented in the literature and is consistent with the sample spectrum of the series.

Figure 1: U.S. quarterly GDP growth rate. Original series, estimated cyclical component, decomposition into two cycles, sample and estimated spectrum.

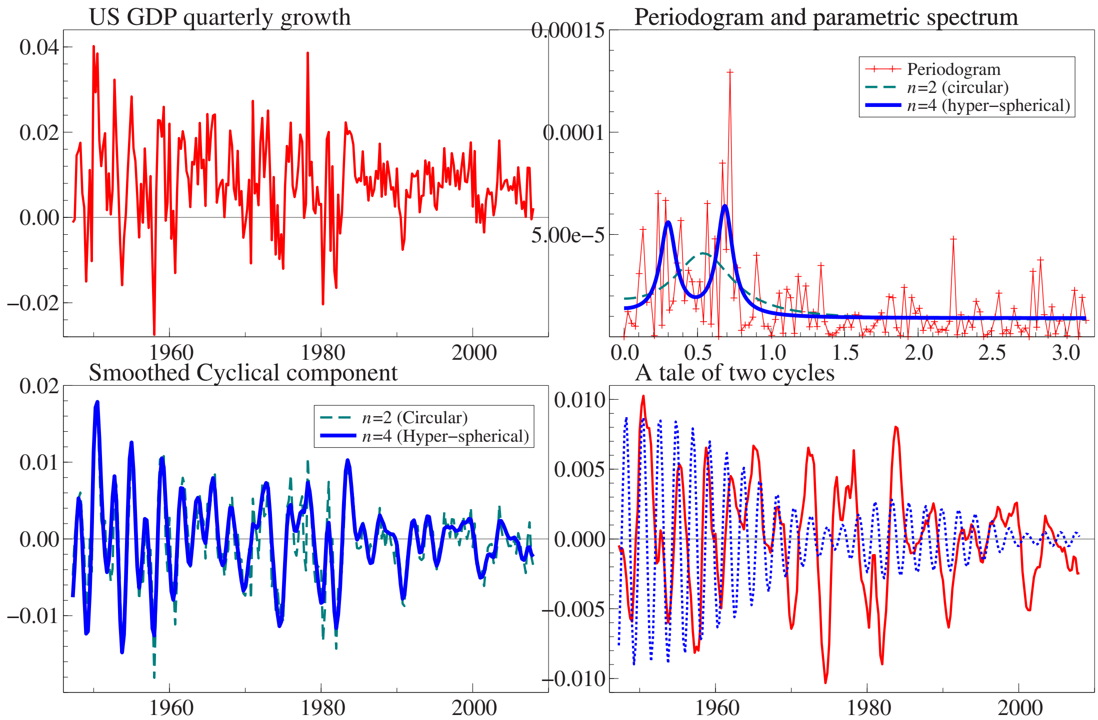

We are now going to fit the model

$$y_t = \mu + \psi_t + \epsilon_t,$$

where $\epsilon_t \sim \text{WN}(0, \sigma^2_\epsilon)$ and ψ_t is the generalized n-dimensional cyclical component given in (10)-(11), with $n = 4$, and compare the results with the HS specification and the circular cycle with $n = 2$. Model selection lead to the cyclical model with $k = 2$ rotation angles and

$$\mathbf{G}(\boldsymbol{\omega}) = \mathbf{G}_{12}(\omega_1)\mathbf{G}_{13}(\omega_1)\mathbf{G}_{14}(\omega_1)\mathbf{G}_{23}(\omega_2)\mathbf{G}_{24}(\omega_2)\mathbf{G}_{34}(\omega_2).$$

The estimation results, presented in table 2, confirm that also for the extended sample the HS specification with two deterministic cycles is preferable, although the BIC would point to the opposite conclusion. The generalized four-dimensional cycle with two frequencies provides the best fit. The estimated

Model	$\hat{\rho}$	$\hat{\omega} \in (0, \pi)$	$\hat{\sigma}^2_\kappa$	$\hat{\sigma}^2_\epsilon$	log-likelihood	AIC	BIC	Ljung-Box (8)
$n = 2$	0.86	0.48	201	1615	-683.62	1377.6	1392.0	6.46
HS	1; 1	0.26; 0.49	0	1884	-677.80	1372.5	1395.3	4.35
$n = 4, k = 2$	1	0.28; 3.00	0	1895	-679.40	1371.3	1388.6	6.75

Table 2: Rainfall in Fortaleza. Estimation results

cycle and its spectral density (logarithms) is plotted are figure 2. The third panel compares the cycle with that arising from the HS model.

5.3 Mink-Muskrat Interaction

Our final illustration is an application of the elliptical cycle model to a famous bivariate time series, relating to the number of skins of minks and muskrats traded annually by the Hudson Bay Company in Canada from 1848 to 1909. The interest in this series lies in the fact that among the two species there is a prey-predator relationship, which a sensible multiple time series model should capture. The series has been extensively investigated and discussed, by Bulmer (1974), Chan and Wallis (1978), Teräsvirta (1985), Zhang, Yao, Tong and Stenseth (2003), among others.

As in Bulmer (1974) and Chan and Wallis (1978), the series are preliminarily transformed into logarithms and detrended by removing a quadratic trend and linear trend respectively from the mink and muskrat series. The detrended series are plotted in figure 3. Denoting the detrended muskrat and mink series respectively by y_{1t}, and y_{2t}, and letting $\mathbf{y}_t = [y_{1t}, y_{2t}]'$, Chan and Wallis (CW) fitted the following vector ARMA(2,1) model with common AR polynomial:

$$\varphi(L)\mathbf{y}_t = \boldsymbol{\Theta}(L)\epsilon_t, \epsilon_t \sim \text{N}(\mathbf{0}, \boldsymbol{\Sigma}),$$

where $\epsilon_t = [\epsilon_{1t}, \epsilon_{2t}]'$. The maximum likelihood estimates of the parameters resulted:

$$\hat{\varphi}(L) = 1 - 1.28L + 0.63L^2, \hat{\boldsymbol{\Theta}}(L) = \begin{bmatrix} 1 - 0.27L & -0.79L \\ 0.34L & 1 - 0.75L \end{bmatrix}, \hat{\boldsymbol{\Sigma}} = \begin{bmatrix} 0.061 & 0.023 \\ 0.023 & 0.054 \end{bmatrix}$$

Figure 2: Annual rainfall series, Fortaleza (Brazil). Original series, estimated signal and cyclical component, and estimated log-spectrum for the model $n = 4, k = 2$.

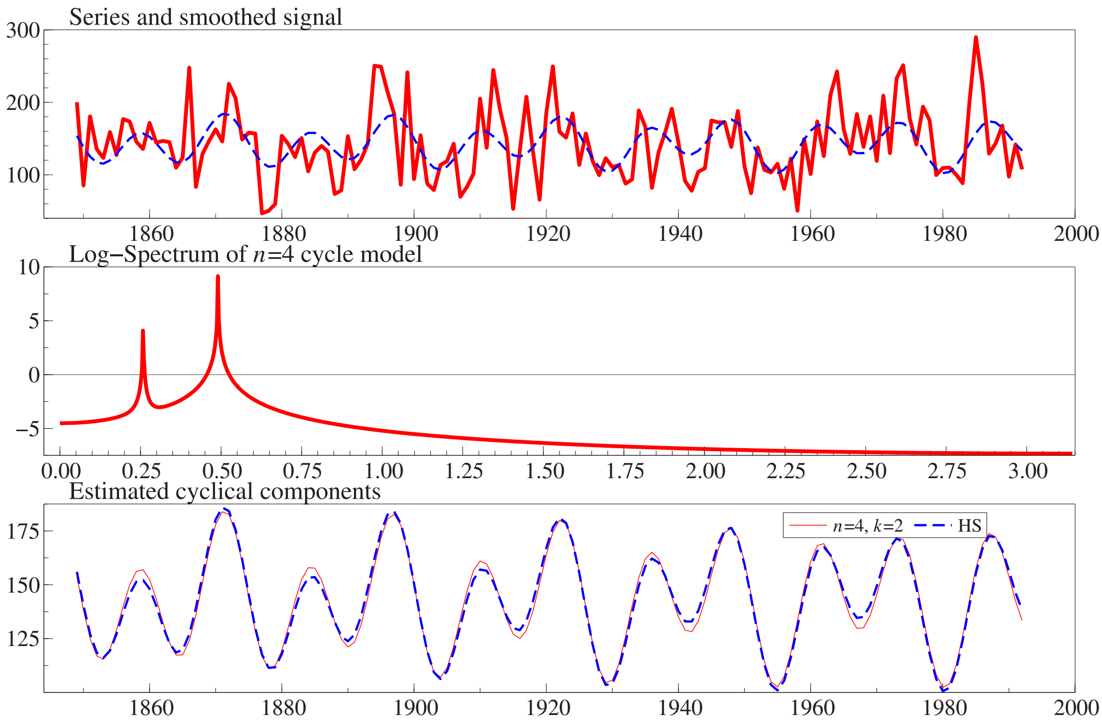

The roots of the AR polynomial are complex and implying a damped oscillation with period 9.93 years. As a measure of predictability, on an reverse scale, we can consider $|\hat{\boldsymbol{\Sigma}}|$, which equals 0.00275.

Since the above model could arise as the final equations form of a vector ARMA model (see Zellner and Palm, 1974), CW proceed to fit the VAR(1) model

$$\boldsymbol{\Phi}(L)\mathbf{y}_t = \epsilon_t, \epsilon_t \sim \mathrm{N}(\mathbf{0}, \boldsymbol{\Sigma}),$$

which is the only VARMA model which can generate the above specification. The estimated coefficients are

$$\hat{\boldsymbol{\Phi}}(L) = \begin{bmatrix} 1 - 0.79L & 0.68L \\ -0.29L & 1 - 0.51L \end{bmatrix} \hat{\boldsymbol{\Sigma}} = \begin{bmatrix} 0.061 & 0.022 \\ 0.022 & 0.058 \end{bmatrix}$$

such that $|\hat{\boldsymbol{\Phi}}(L)| = 1 - 1.30L + 0.60L^2$, which implies an AR(2) and conclude that the VAR(1) specification provides a parsimonious and yet essential account of the interactions of the two series. In particular, the off-diagonal AR coefficients imply that an increase in the muskrat population (prey) is followed by an increase in the mink population (predator) a year later, and an increase in mink is followed by a decrease in muskrat a year later. The estimated model implies that the two series display a cycle with a period of about 10 years, with the muskrat cycle leading the mink cycle by 2.4 years. With respect to the original specification, the VAR(1) model yields an higher value of the (un)predictability, $|\hat{\boldsymbol{\Sigma}}|$, which now equals 0.00305, but has fewer parameters.

In the place of an unrestricted VAR(1) model we fit and compare two bivariate cycle models, the spherical cycle model (SCM) and the elliptical (ECM), which can be regarded as two constrained version of the final model fitted by CW. The SCM is specified as follows:

$$\mathbf{y}_t = \rho \mathbf{G}_{12}(\omega)\mathbf{y}_{t-1} + \boldsymbol{\epsilon}_t, \epsilon_t \sim \mathrm{N}(\mathbf{0}, \boldsymbol{\Sigma}),$$

whereas the ECM is

$$\mathbf{y}_t = \mathbf{E}(\omega)\mathbf{y}_{t-1} + \boldsymbol{\epsilon}_t, \epsilon_t \sim \mathrm{N}(\mathbf{0}, \boldsymbol{\Sigma}),$$

where was given in 5, i.e.

$$\mathbf{E}(\omega) = \begin{bmatrix} \alpha \cos \omega & \alpha \sin \omega \\ -\beta \sin \omega & \beta \cos \omega \end{bmatrix}.$$

Therefore, the ECM encompasses the SCM, which arises when $\alpha = \beta (= \rho)$.

Table 3 displays some estimation results. The estimated values of α and β resulted respectively 1.00 and 0.60, whereas the cycle frequency is estimated equal to 0.63. The hypothesis $H_0 : \alpha = \beta$ is strongly rejected. The results provide strong support for the elliptical cycle specification. The second panel of figure 3 suggest that this is the case since the variability of muskrat population is larger than that characterizing minks, so that the time plot of y_{2t} versus y_{1t} has an elliptical, rather than circular, shape.

Model	$\hat{\omega} \in (0, \pi)$	$\hat{\varphi}(L)$	log-lik	AIC	BIC	$\|\mathbf{\Sigma}\|$
SCM	0.45	$1 - 1.46L + 0.66L^2$	-2.59	20.0	38.9	0.00359
ECM	0.69	$1 - 1.29L + 0.60L^2$	3.04	11.0	32.5	0.00301

Table 3: Mink-Muskrat bivariate time series. Estimation results

The estimated autoregressive matrix polynomial and prediction error covariance matrix for the ECM are very similar to the unrestricted VAR(1) model fitted by CW:

$$\mathbf{I} - \mathbf{E}(\omega)L = \begin{bmatrix} 1 - 0.81L & 0.59L \\ -0.36L & 1 - 0.49L \end{bmatrix}, \hat{\mathbf{\Sigma}} = \begin{bmatrix} 0.061 & 0.021 \\ 0.021 & 0.056 \end{bmatrix}.$$

The implied final equations form has $\hat{\varphi}(L) = |\mathbf{I}_2 - \hat{\mathbf{E}}(\omega)L|$ almost identical to that implied by CW's VAR(1) model (see table 3), and the predictability measure is about the same (actually, it is slightly smaller). Moreover, it has a parameter less and thus ECM would be preferred to the VAR(1) by an information criterion.

The bottom right hand panel of figure 3 displays the two parametric spectra implied for the two series by the ECM specification, which have the following expressions. Denoting by σ_{ij} the generic element of $\mathbf{\Sigma}$,

$$f_{11}(\lambda) = \frac{1}{2\pi} \frac{\sigma_{11}(1 - 2\beta\cos\omega\cos\lambda + \beta^2\cos^2\omega) + \sigma_{12}(2\alpha\sin\omega\cos\lambda - \alpha\beta\sin 2\omega) + \sigma_{22}(\alpha^2\sin^2\omega)}{1 + \alpha^2\beta^2 + (\alpha+\beta)^2\cos^2\omega - 2(\alpha+\beta)(1+\alpha\beta)\cos\omega\cos\lambda + 2\alpha\beta\cos(2\lambda)},$$

$$f_{22}(\lambda) = \frac{1}{2\pi} \frac{\sigma_{11}(\beta^2\sin^2\omega) + \sigma_{12}(\alpha\beta\sin 2\omega - 2\beta\sin\omega\cos\lambda) + \sigma_{22}(1 - 2\alpha\cos\omega\cos\lambda + \alpha^2\cos^2\omega)}{1 + \alpha^2\beta^2 + (\alpha+\beta)^2\cos^2\omega - 2(\alpha+\beta)(1+\alpha\beta)\cos\omega\cos\lambda + 2\alpha\beta\cos(2\lambda)}.$$

The spectral peak is located at a frequency corresponding to a ten year cycle.

The last panel shows the spectral coherence and the phase between the two series, computed respectively as $\Re\{f_{12}(\lambda)\}^2 + \Im\{f_{12}(\lambda)\}^2$ and $\arctan\{-\Im\{f_{12}(\lambda)\}/\Re\{f_{12}(\lambda)\}\}$ where $\Re$ and $\Im$ are the real and imaginary parts of the cross-spectrum:

$$f_{12}(\lambda) = \frac{1}{2\pi} \frac{\sigma_{11}s_{11} + \sigma_{12}s_{12} + \sigma_{22}s_{22}}{1 + \alpha^2\beta^2 + (\alpha+\beta)^2\cos^2\omega - 2(\alpha+\beta)(1+\alpha\beta)\cos\omega\cos\lambda + 2\alpha\beta\cos(2\lambda)},$$

where $s_{11} = -\beta\sin\omega e^{\imath\lambda} + \beta^2\sin\omega\cos\omega$, $s_{12} = 1 - \cos\omega(\alpha e^{\imath\lambda} + \beta e^{-\imath\lambda}) + \alpha\beta\cos 2\omega$, $s_{22} = \alpha\sin\omega e^{-\imath\lambda} - \alpha^2\sin\omega\cos\omega$.

6 Conclusions

The paper has proposed multivariate and elliptical extensions of the traditional circular cycle model. The empirical applications have pointed out under what circumstances these extensions can be fruitful. Other potential applications deal with the parametric estimation of the spectral density of a stationary stochastic process characterized by multiple peaks.

Figure 3: Mink-Muskrat bivariate time series. Original series, phase plot, univariate spectra, coherence and phase diagram implied by the elliptical cycle model.

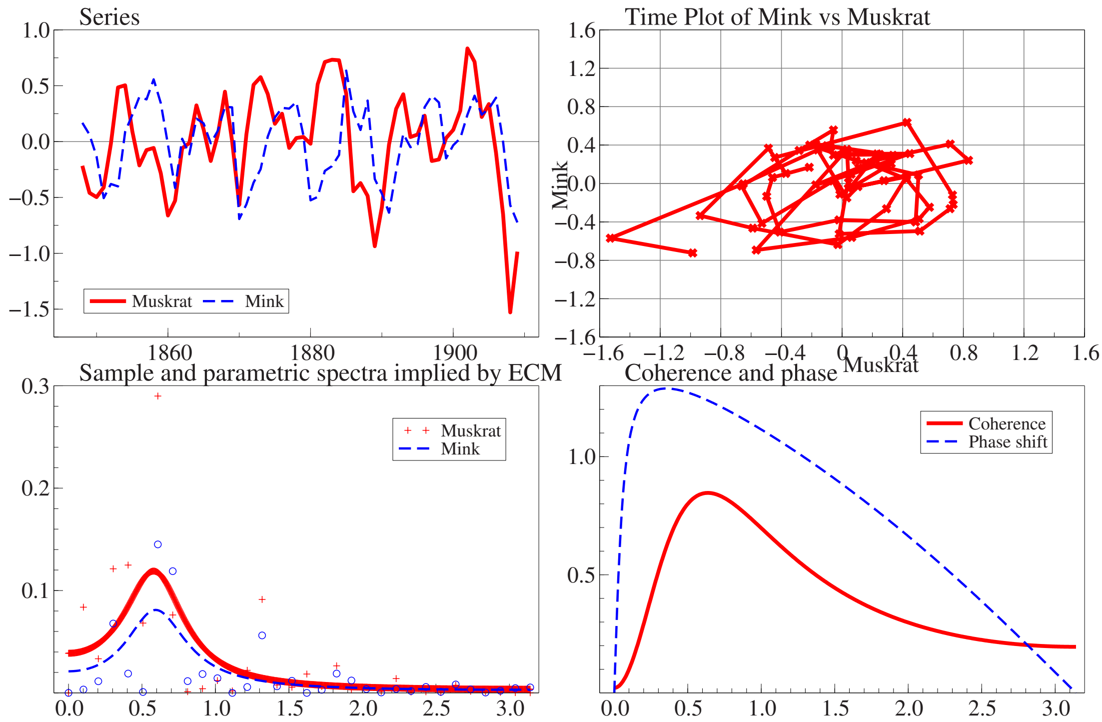

There are some open issues that this paper has left unresolved and that we leave for future research. The first deals with the relationship between the rotation angles ω_{ij} and the spectral peaks ζ_h. Apart from very special cases, it is not possible to derive the distribution of the ζ_h's from that of the ω_{ij}'s. The second deals with the multivariate extension of the elliptical model, which would be relevant for modeling the cyclical interactions in multiple time series.

Appendix

A Proof of Proposition 1

We aim at locating the value of λ for which the power spectrum of the circular stochastic cycle (1),

$$f(\lambda) = \frac{\sigma_k^2}{2\pi} \frac{1+\rho^2 - 2\rho\cos\omega\cos\lambda}{1+\rho^4+4\rho^2\cos^2\omega - 4\rho(1+\rho^2)\cos\omega\cos\lambda + 2\rho^2\cos(2\lambda)},$$

is maximum. First notice that

$$\lim_{\rho\to 0} f(\lambda) = \frac{\sigma_k^2}{2\pi} \quad \text{and} \quad \lim_{\rho\to 1} f(\omega) = \infty,$$

since the (squared) denominator of the above equation is null for

$$\cos\lambda = \frac{(1+\rho^2)\cos\omega \mp \sin\omega\sqrt{-(1-\rho^2)^2}}{2\rho},$$

i.e. for $\rho = 1$ and $\lambda = \omega$. When $\rho \in (0,1)$, the first order conditions give:

$$\begin{aligned} & 2\rho\cos\omega\sin\lambda(1+\rho^4+4\rho^2\cos^2\omega - 4\rho(1+\rho^2)\cos\omega\cos\lambda + 2\rho^2\cos(2\lambda)) + \\ - \quad & (4\rho(1+\rho^2)\cos\omega\sin\lambda - 4\rho^2\sin(2\lambda))(1+\rho^2-2\rho\cos\omega\cos\lambda) = 0. \end{aligned}$$

Equivalently

$$\begin{aligned} & \sin\lambda\left[2\rho\cos\omega(1+\rho^4+4\rho^2\cos^2\omega) - (2\rho\cos\omega)4\rho(1+\rho^2)\cos\omega\cos\lambda + \right. \\ + \quad & \left.(2\rho\cos\omega 2\rho^2\cos(2\lambda)) - (4\rho(1+\rho^2)\cos\omega - 4\rho^2 2\cos(\lambda))(1+\rho^2-2\rho\cos\omega\cos\lambda)\right] = 0, \end{aligned}$$

which is null for $\lambda = 0$ (this is a relative minimum). Let us consider the other solutions. By some algebra, the above equation can be written as the second order equation in $\cos\lambda$,

$$4\rho^2\cos\omega\cos^2\lambda - 2\rho(1+\rho^2)2\cos\lambda - \cos\omega(1+\rho^4+4\rho^2\cos^2\omega) + 2\rho^2\cos\omega + 2(1+\rho^2)^2\cos\omega = 0.$$

Noticing that $-1-\rho^4-6\rho^2 = -(1+\rho^2)^2 - 4\rho^2$ and using some algebra and trigonometric identities, one can obtain the roots of the above equations as

$$\cos\lambda_{1,2} = \frac{(1+\rho^2) \mp \sin\omega\sqrt{(1+\rho^2)^2 - 4\rho^2\cos^2\omega}}{2\rho\cos\omega}$$

The quantity under square root is always positive for $\rho < 1$ and there is only one admissible solution, in modulus smaller than one, that can be expressed as

$$\cos\lambda_{max} = \frac{1+\rho^2}{2\rho\cos\omega}\left(1 - \sin\omega\sqrt{1 - \frac{4\rho^2}{(1+\rho^2)^2}\cos^2\omega}\right).$$

The overall conclusion is that, for ρ that tends to unity, the spectrum reaches its maximum at a frequency λ that tends to the frequency of the cycle, ω. As long as ρ decreases, the maximum of the spectrum is attained for values of $\lambda < \omega$.

B Proof of Proposition 2

The proof is analogue to the proof of proposition 1, provided that α and β are considered in place of ρ, so we just summarise the main steps. Differentiating (6) with respect to λ and equating to zero gives

$$\sin\lambda(8\alpha\beta^2\cos\omega\cos^2\lambda - 2A\cos\lambda - B) = 0,$$

where $A = 4\alpha\beta(1+R^2)$, $B = 2\beta\cos\omega(1+\alpha^2\beta^2+(\alpha+\beta)^2\cos^2\omega - 2\beta) - 2(\alpha+\beta)(1+\alpha\beta)(1+R^2)\cos\omega)$ and $R^2 = \alpha^2\sin^2\omega + \beta^2\cos^2\omega$, from which the relative minimum in $\lambda = 0$. Solving the second order equation in $\cos\lambda$ gives

$$\cos\lambda_{max} = \frac{1+R^2}{2\beta\cos\omega}\left(1 \mp \sqrt{1 + C\cos^4\omega - D\cos^2\omega}\right),$$

where $C = \frac{\beta}{\alpha}\frac{(\alpha+\beta)^2}{(1+R^2)^2}$, $D = -\left(\frac{\frac{\beta}{\alpha}+\alpha\beta^3-2\beta^2}{(1+R^2)^2} - \frac{1+\alpha\beta+\frac{\beta}{\alpha}+\beta^2}{1+R^2}\right)$, $C, D > 0$. Of the two solutions, only the one with the minus gives a value for the cosine which is smaller than one. Using trigonometric identities and collecting terms, we rewrite the above equation to have the solution given in proposition 4.

C Proof of Proposition 3

To obtain the reduced form of ψ_t in (8), we start by writing

$$\boldsymbol{\psi}_t = \mathbf{Z}'\rho\mathbf{G}_z(\xi)\mathbf{Z}\boldsymbol{\psi}_{t-1} + \boldsymbol{\kappa}_t$$

which, after some algebra, is equivalent to

$$\tilde{\boldsymbol{\psi}}_t = \frac{(\mathbf{I} - \rho\mathbf{G}_z(\xi)L)^*}{\det(\mathbf{I} - \rho\mathbf{G}_z(\xi)L)}\boldsymbol{\kappa}_t,$$

where $\tilde{\boldsymbol{\psi}}_t = \mathbf{Z}\boldsymbol{\psi}_t$ and the superscript * denotes the adjoint, or adjugate, of a matrix. The above expression allows us to conveniently derive the reduced form of the reparameterized process $\tilde{\boldsymbol{\psi}}_t$. In fact, for all the components of $\tilde{\boldsymbol{\psi}}_t$, i.e. the processes $\tilde{\psi}_t$, $\tilde{\psi}_t^\dagger$ and $\tilde{\psi}_t^\ddagger$, the autoregressive polynomial is $\det(\mathbf{I} - \rho\mathbf{G}_z(\xi)L) = (1-\rho L)(1 - 2\rho\cos\xi L + \rho^2L^2)$, whereas the moving average polynomial is the j-th row of $(\mathbf{I} - \rho\mathbf{G}_z(\xi)L)^*$, for $j = 1, 2, 3$. The adjoint is here obtained as

$$(\mathbf{I} - \rho\mathbf{G}_z(\xi)L)^* = p_1\mathbf{I} + p_2(\mathbf{I} - \rho\mathbf{G}_z(\xi)L) + p_3(\mathbf{I} - \rho\mathbf{G}_z(\xi)L)^2$$

where the p_j are the coefficients of x^j in the characteristic polynomial $p(x) = |(\mathbf{I} - \rho\mathbf{G}_z(\xi)L) - x\mathbf{I}|$, i.e.

$$\begin{aligned}
p_1 &= 3 + \rho^2L^2 + 2\rho^2\cos\xi L^2 - 4\rho\cos\xi L - 2\rho L \\
p_2 &= 2\rho\cos\xi L + \rho L - 3 \\
p_3 &= 1,
\end{aligned}$$

which follows by the Cayley-Hamilton theorem ($p(\mathbf{I}-\rho\mathbf{G}_z(\xi)L)=\mathbf{0}$) and by the fact that $p_0=-|\mathbf{I}-\rho\mathbf{G}_z(\xi)L|$ (Lancaster and Tismenetsky, p. 157, Theorem 2, and p. 165, Ex. 8). With some algebra,

$$(\mathbf{I}-\rho\mathbf{G}_z(\xi)L)^*=\mathbf{I}+\left[(1+2\cos\xi)(\mathbf{I}-\mathbf{G}_z(\xi))+\mathbf{G}_z(\xi)^2\right]\rho^2L^2-\left[(1+2\cos\xi)\mathbf{I}-\mathbf{G}_z(\xi)\right]\rho L$$

whose first row times $\boldsymbol{\kappa}_t$ is equal to

$$\begin{aligned}\mathbf{e}_1'(\mathbf{I}-\rho\mathbf{G}_z(\xi)L)^*\boldsymbol{\kappa}_t &= \{1-(1+\cos\xi)\rho L+[(1+2\cos\xi)(1-\cos\xi)+\cos(2\xi)]\,\rho^2L^2\}\kappa_t+\\ &\quad+\{\rho\sin\xi L+[-(1+2\cos\xi)\sin\xi+\sin(2\xi)]\,\rho^2L^2\}\kappa_t^\dagger,\end{aligned}$$

where $\mathbf{e}_1=[1\ 0\ 0]'$. Hence, the reduced form of $\tilde{\psi}_t$ is

$$(1-\rho L)(1-2\rho\cos\xi L+\rho^2L^2)\tilde{\psi}_t=\{1-(1+\cos\xi)\rho L+\cos\xi\rho^2L^2\}\kappa_t+\{\rho\sin\xi L-\sin\xi\rho^2L^2\}\kappa_t^\dagger.$$

Collecting terms we find

$$(1-\rho L)(1-2\rho\cos\xi L+\rho^2L^2)\tilde{\psi}_t=(1-\rho L)(1-\cos\xi\rho L)\kappa_t+(1-\rho L)(\rho\sin\xi L)\kappa_t^\dagger,$$

i.e., $\tilde{\psi}_t$ is observationally equivalent to the first order stochastic cycle (1).

The reduced form of the auxiliary processes $\tilde{\psi}_t^\dagger$ and $\tilde{\psi}_t^\ddagger$ are derived in an analog way and are given by the ARMA(2,1) process $(1-2\rho\cos\xi L+\rho^2L^2)\tilde{\psi}_t^\dagger=-(\rho\sin\xi L)\kappa_t+(1-\cos\xi\rho L)\kappa_t^\dagger$ and the AR(1) process $(1-\rho L)\tilde{\psi}_t^\ddagger=\kappa_t^\ddagger$, respectively.

Finally, $\psi_t=\mathbf{e}_1'\mathbf{Z}'\tilde{\boldsymbol{\psi}}_t$ is the ARMA(3,2) process given in (9). The spectrum is obtained by the Fourier transform of the spectral generating function for an ARMA process, see Harvey (1989, pag. 59). This concludes the proof of proposition 2.

D Proof of Proposition 4

Let us write (10) as

$$\boldsymbol{\psi}_t=\frac{(\mathbf{I}-\rho\mathbf{G}(\boldsymbol{\omega})L)^*}{\det(\mathbf{I}-\rho\mathbf{G}(\boldsymbol{\omega})L)}\boldsymbol{\kappa}_t.$$

If n is even, then $\det(\mathbf{I}-\rho\mathbf{G}(\boldsymbol{\omega})L)=\prod_{h=1}^{\frac{n}{2}}(1-2\rho\cos\zeta_hL+\rho^2L^2)$ which follows by the fact that the spectrum of $\mathbf{G}(\boldsymbol{\omega})$ is the set $\{e^{\imath\zeta_1},e^{\imath\zeta_2},\dots,e^{\imath\zeta_n}\}$, where $\zeta_{2h}=-\zeta_{2h-1}$, for $h=1,2,\dots,\frac{n}{2}$, and $\mathrm{tr}(\mathbf{G}(\boldsymbol{\omega}))=2\sum_{h=1}^{\frac{n}{2}}\cos\zeta_h$. The adjoint is

$$(\mathbf{I}-\rho\mathbf{G}(\boldsymbol{\omega})L)^*=-\sum_{j=1}^{n}(-1)^{n-j}s_{n-j}(\mathbf{I}-\rho\mathbf{G}(\boldsymbol{\omega})L)^{j-1},$$

where we have used the Cayley-Hamilton theorem, as in the proof of proposition 3, with $p_j=(-1)^{n-j}s_{n-j}$ and s_{n-j} being the symmetric function of the eigenvalues of $\mathbf{I}-\rho\mathbf{G}(\boldsymbol{\omega})L$, defined to be the sum of the product of the eigenvalues taken $n-j$ at a time, i.e.

$$s_{n-j}=\sum_{1\le i_1<i_2<\ldots<i_{n-j}\le n}(1-\rho e^{\imath\zeta_{i_1}}L)(1-\rho e^{\imath\zeta_{i_2}}L)\ldots(1-\rho e^{\imath\zeta_{i_{n-j}}}L)$$

(Meyer, 2000, p. 494). Writing $(\mathbf{I}-\rho\mathbf{G}(\boldsymbol{\omega})L)^{j-1} = \mathbf{V}(\mathbf{I}-\rho\boldsymbol{\Xi}L)^{j-1}\mathbf{V}^H$, where $\boldsymbol{\Xi} =$ diag $(e^{\imath\zeta_1}, e^{\imath\zeta_2}, \dots, e^{\imath\zeta_n})$, and taking the first row, we obtain (12).

If n is odd, then the spectrum of $\mathbf{G}(\boldsymbol{\omega})$ is the set $\{e^{\imath\zeta_1}, e^{\imath\zeta_2}, \dots, e^{\imath\zeta_{n-1}}, 1\}$, where $\zeta_{2h} = -\zeta_{2h-1}$, for $h = 1, 2, \dots, \frac{n-1}{2}$ with tr$(\mathbf{G}(\boldsymbol{\omega})) = 1+2\sum_{h=1}^{\frac{n-1}{2}} \cos\zeta_h$, the adjoint is $(\mathbf{I}-\rho\mathbf{G}(\boldsymbol{\omega})L)^* = \sum_{j=1}^{n}(-1)^{n-j}s_{n-j}(\mathbf{I}-\rho\mathbf{G}(\boldsymbol{\omega})L)^{j-1}$ and, consequently,

$$(1-\rho L)\prod_{h=1}^{\frac{n-1}{2}}(1-2\rho\cos\zeta_h L+\rho^2L^2)\psi_{t,1} = \sum_{j=1}^{n}\sum_{i=1}^{n}\sum_{k=1}^{n}(-1)^{n-j}s_{n-j}v_{1i}(1-\rho e^{\imath\zeta_i}L)^{j-1}\overline{v}_{ki}\kappa_{t,k},$$

provided that $\zeta_n = 0$. The spectra are obtained through the spectral generating function for an ARMA process, see Harvey (1989, pag. 59).

References

Bulmer M.G. (1974), A statistical analysis of the 10-year cycle in Canada, *Journal of Animal Ecology*, 43, 701718.

Chan W.-Y. T. and Wallis K.F. (1978), Multiple Time Series Modelling: Another Look at the Mink-Muskrat Interaction, *Applied Statistics*, 27, 2, 168-175.

Doornik, J.A. (2006), *Ox. An Object-Oriented Matrix Programming Language*, Timberlake Consultants Press, London.

Durbin, J., Koopman S.J. (2001), *Time Series Analysis by State Space Methods*, Oxford University Press.

Givens W. (1958), Computation of plane unitary rotations transforming a general matrix to triangular form, *SIAM Journal*, 6, 1, 2650.

Goldstein H. (1980), *Classical Mechanics*, second edition, Addison-Wesley.

Golub G.H. and van Loan C.F. (1996), *Matrix Computations*, third edition, The John Hopkins University Press.

Gray, S., Zhang, N.-F., Woodward, W.A., 1989. On generalized fractional processes. *Journal of Time Series Analysis*, 10, 233-257.

Hannan E.J. (1964), The Estimation of a Changing Sesasonal Pattern, *Journal of the American Statistical Association*, 59, 308, 1063-1077.

Harvey A.C. (1985), Trends and Cycles in Macroeconomic Time Series, *Journal of Business and Economics Statistics*, 3, 3, 216-227.

Harvey A.C. (1989), *Forecasting, Structural Time Series Models and the Kalman Filter*, Cambridge University Press.

Harvey A.C. and Jaeger A. (1993), Detrending, Stylized Facts and the Business Cycle, *Journal of Applied Econometrics*, 8, 231-247.

Harvey A.C. and Souza R.C. (1987), Assessing and Modeling the Cyclical Behavior of Rainfall in Northeast Brazil, *Journal of Climate and Applied Meteorology*, 26, 10, 1339-1344.

Harvey A.C. and Trimbur, T.M. (2003), General Model-based Filters for Extracting Cycles and Trends in Economic Time Series, *The Review of Economics and Statistics*, 85, 2, 244-255.

Haywood J. and Tunnicliffe Wilson, G. (2000), An Improved State Space Representation for Cyclical Time Series, *Biometrika*, 87, 3, 724-726.

Kendall M.G. (1945), On the Analysis of Oscillatory Time-Series, *Journal of the Royal Statistical Society, Series B*, 108, 1/2, 93-141.

Koopman S.J., Harvey, A.C., Doornik, J.A. and Shephard, N. (2006), *STAMP: Structural Time Series Analyser, Modeller and Predictor*, Timberlake Consultants Press.

Lancaster P. and Tismenetsky M. (1985), *The Theory of Matrices*, Academic Press.

Lütkepohl H. (2006), *New Introduction to Multiple Time Series Analysis*, Springer.

Meyer C.D. (2000), *Matrix Analysis and Applied Linear Algebra*, SIAM.

Morgan M.S. (1990), *The History of Econometric Ideas*. Cambridge University Press, Cambridge, U.K.

Morley J.C., Nelson C.R., Zivot E. (2003), Why Are the Beveridge-Nelson and Unobserved Components Decompositions of GDP So Different?, *The Review of Economics and Statistics*, 85, 2, 235-243.

Teräsvirta, T. (1985), Mink and Muskrat interaction: a structural approach, *Journal of Time Series Analysis*, 6, 3, 171-180.

Tong H., Lim K.S. (1980), Threshold Autoregression, Limit Cycles and Cyclical Data, *Journal of the Royal Statistical Society, Series B*, 42, 3, 249-292.

Trimbur, T.M. (2005), Properties of Higher Order Stochastic Cycles, *Journal of Time Series Analysis*, 27, 1, 1-17.

West, M., Harrison, J. (1989), *Bayesian Forecasting and Dynamic Models*, 1st edition, New York, Springer-Verlag.

West, M., Harrison, J. (1997), *Bayesian Forecasting and Dynamic Models*, 2nd edition, New York, Springer-Verlag.

Yule, G.U. (1927), On a Method of Investigating Periodicities in Disturbed Series, with Special Reference to Wolfer's Sunspot Numbers, *Philosophical Transactions of the Royal Society of London. Series A, Containing Papers of a Mathematical or Physical Character*, 226, 1, 267-298.

Zellner A., Palm F. (1974), Time series analysis and simultaneous equation econometric models, *Journal of Econometrics*, 2, 1754

Zhang W., Yao Q., Tong H.,Stenseth N.C. (2003), Smoothing for Spatiotemporal Models and Its Application to Modeling Muskrat-Mink Interaction, *Biometrics*, 59, 4, 813-821.